arXiv:1401.7921v2 [physics.bio-ph] 15 Jul 2014

Catastrophic shifts and lethal thresholds in a propagating front model of unstable tumor progression

Daniel R. Amor[1,2], Ricard V. Solé[1,2,3]
[1] *ICREA-Complex Systems Lab, Universitat Pompeu Fabra, Dr. Aiguader 80, 08003 Barcelona, Spain*
[2] *Institut de Biologia Evolutiva, CSIC-UPF, Psg Barceloneta, Barcelona, Spain*
[4] *Santa Fe Institute, 1399 Hyde Park Road, New Mexico 87501, USA*

Unstable dynamics characterizes the evolution of most solid tumors. Because of an increased failure of maintaining genome integrity, a cumulative increase in the levels of gene mutation and loss is observed. Previous work suggests that instability thresholds to cancer progression exist, defining phase transition phenomena separating tumor-winning scenarios from tumor extinction or coexistence phases. Here we present an integral equation approach to the quasispecies dynamics of unstable cancer. The model exhibits two main phases, characterized by either the success or failure of cancer tissue. Moreover, the model predicts that tumor failure can be due to either a reduced selective advantage over healthy cells or excessive instability. We also derive an approximate, analytical solution that predicts the front speed of aggressive tumor populations on the instability space.

PACS numbers: 89.75.Fb, 89.70.+c, 89.75.Hc, 89.75.-k, 89.75.Kd

I. INTRODUCTION

Cancer is a disease that can be initiated by the failure of a single cell. Whenever such failure leads to some proliferation advantage over the neighboring somatic cells, this single cell is prone to originate its own cell lineage within its host tissue. After many rounds of replication, additional failures may occur, eventually generating a large population of abnormal, proliferating cells. This would be a rough description of the disease, but it would be more appropriate to say that cancer is an evolutionary dynamic process [1,2]. Changes occur in time and accumulate over generations and the final success of the tumor requires an appropriate accumulation of changes affecting different types of genes.

We can classify cancer genes into three basic categories [3]: (a) oncogenes, (b) tumor suppressor genes and (c) stability-related genes. These groups corresponds to genes that (a) increase replication due to mutation, (b) increase cell growth when the gene is silenced or lost and (c) modify genome stability due to failures in cell division, repair and maintenance mechanisms [4-9]. All these changes occur through the process of cell replication, when cancer genes are likely to experience mutations or losses [10] leading to the emergence of fitter mutant clones.

In order to understand the evolution of cancer, a huge amount of mathematical models have analyzed the impact of selection [11] on the evolution of clones. The stochasticity of mutations has also been shown to play a major role in triggering the clonal competition among different mutants, and could be a principal reason for the high heterogeneities (and the long waiting time to malignancy) observed in cancer development [12]. Another very relevant mechanism is spatial structure, which is also very significant in many ecological and evolutionary processes [13]. For example, in the context of asexual evolving populations, the spatial competition between different clones slows down the establishment of driver mutations (i. e. mutations causing a selective advantage) [14] if the population exceeds a critical size. Analogous results have been found in the context of cancer evolution, where space can increase the waiting time to tumor malignancy [15]. In other cases, the spatial invasion of tumors has been modeled as a propagating front [16]. This has permitted to, e.g., compare the role of advection (chemotaxis) and cell diffusion on the invasion speed of glioblastomas [17,18], or analyze the invasiveness enhancement by acidic pH gradients at tumor-host interfaces [19].

Although most classic models of cancer evolution deal with those factors associated with growth and competition among clones, a specially important characteristic of most tumors is precisely the increased levels of instability associated to progression. Instability can be understood in terms of mutations but also of losses and gains of genetic components that modify genome stability, making cells more prone to errors while replicating [20]. Mutations have been an intrinsic part of all evolutionary models of population dynamics (including cancer) but it is typically assumed that mutation rate remains constant over time. In genomically unstable tumors, the failure of the repair mechanisms, along with the generation of aneuploidy, makes possible to damage key components associated to the maintenance of genome integrity [4-9,20].

With their loss or failure, further increases of instability are expected to occur, since other genes linked to stability and repair are more likely to be damaged. As a consequence, instability itself can evolve over time. Such evolvable trait raises the question of how much instability can accumulate through carcinogenesis. It has been suggested that optimal instability rates [4] as well as thresholds to instability exist. The latter define the transition boundaries between viable and non-viable cancer populations [21-24]. There are actually examples of

phase transitions defining the boundaries of viability in RNA viruses[25-30]. RNA virus populations are quasispecies [22,30] i.e. highly heterogeneous, related genotypes. Critical thresholds of mutation have been predicted and later experimentally tested [31-33] using invitro scenarios. The presence of such critical transitions have also received a great interest from the field of statistical physics. The nature of the resulting phase transitions have been analyzed for several fitness landscapes, both for finite-size competing molecules [34] and in the limit of infinitely large chains [35]. Error thresholds have also been reported in asexual evolutionary scenarios beyond the RNA viruses. Remarkably, it has been reported that natural selection, favoring immediate fitness benefits, may permit the hitchhiking of deleterious mutations that will finally lead to the population's extinction in the long term[36].

The similarities between unstable cancer and RNA viruses suggests a therapeutically very interesting possibility: the use of additional instability as anticancer therapy [23,37]. That means that, instead of trying to decrease the tumor cells' mutagenesis, an attempt to increase it towards non-viable levels could be a suitable way to fight the disease. Due to the qualitatively sharp change associated to the presence of instability thresholds, a physics approach to phase transitions in cancer quasispecies can be successfully used [23,24,38-40]. In this paper we explore the dynamics and phases of unstable cancer by constructing an analytical model of tumor progression to be defined as a front propagation problem [41] in the space of instability. By using this approximation we provide a better and easily extendable formal description of tumors that allows to characterize both the presence of transitions and the population structure that emerges in each phase. It also provides a well defined, formal approach to predict the speed of cancer propagation.

The paper is organized as follows. In section II we present the rationale for the presence of a phase transition phenomenon separating a phase where the tumor will fail to succeed due to a high instability from another phase where it is expected to win. In section III we revisit the previous linear, discrete model of cancer cells dynamics and we explain some of its limitations. Section IV is devoted to present the integral model of unstable cancer, that improves the previous mathematical description of the disease. Section V presents several scenarios for tumor evolution predicted by the integral model (an analysis of the resulting phase space is included). In section VI we derive an approximate, analytical expression for the tumor front speed on the instability space, and we compare it with some numerical solutions for the model equations. The last section is devoted to discuss the potential implications of our results.

II. TRANSITIONS IN TUMOR INSTABILITY

In order to provide a rationale for the existence (and potential implications) of instability thresholds, let us first consider a mean field, two-compartment model of unstable cancer dynamics. In this model the population will be composed of two cell species, namely, host cells H and cancer cells C. If we indicate as r_n and r_c the rates of growth of normal (host) and cancer cells, respectively, we can write the following evolution equations:

$$\frac{dH}{dt} = r_n H - H\phi(H,C) \quad (1)$$

$$\frac{dC}{dt} = r_c C - C\phi(H,C), \quad (2)$$

where $\phi(H,C)$ is an outflow term that represents the competition between both species. If we consider that the overall cell population $H+C$ is constant (because cells fill a given fixed space) the function ϕ reads $\phi = r_n H + r_c C$ which is actually the average rate of growth.

The following step consists in defining the growth rates for each species. Regarding normal cells, it is sensible to assume a constant growth rate r_n (normal cells are renewed in a stable way to ensure that body functions are properly carried on). The situation is different for cancer cells, for which their average growth rate r_c will depend on how much mutations have been accumulated in the cells' genome. Concretely, the growth rate r_c can be increased by the effects of driver mutations (i.e., mutations promoting cell replication) or decreased by deleterious mutations. Let us denote μ as the probability that a mutation takes place when replicating a given gene. Thus, μ is a measure of the genetic instability of the population. Consider that there exist a number N_r of growth-related genes. If a growth-related gene is damaged (mutated) during the cell replication process, an average increase δ_r in the growth rate is expected. Thus, the average increase in r_c due to driver mutations affecting our cancer population is simply:

$$f_1(\mu) = N_r \mu \delta_r. \quad (3)$$

Similarly, we should expect a decrease in the growth rate due to the potential damage produced if a house keeping gene is damaged or lost. If N_h indicates the number of such genes, the probability that no one is damaged will read

$$f_2(\mu) = (1-\mu)^{N_h}. \quad (4)$$

Available estimates indicate that $N_h \sim 500 - 600$ essential genes exist [42] whereas N_r can be smaller or higher depending on the type of cancer considered. Around one percent of genes in the human genome appear related to the emergence of cancer [43].

In the above eqs. (3) and (4) we have assumed that the mutation and replication rates are the same for all genes, as well as a constant fitness benefit δ_r from driver

mutations. Obviously, this is only simple approach to the more complex reality in which each gene mutates with a different probability and provides a different fitness benefit (or loss). Thus, the final rate of replication will be the product:

$$r_c(\mu) = f_1(\mu) f_2(\mu) = (r_n + \mu N_r \delta r)\,(1-\mu)^{N_h}, \qquad (5)$$

where we have assumed that, in the absence of genetic instability ($\mu = 0$) the normal cells replication rate r_n is recovered. The above function (5) has a maximum at a given optimal instability rate. This is shown in Fig. 1, where we plot $r_c(\mu)$ for a given combination of parameters. The maximum is achieved at an optimal instability level $\mu_o \approx 1/N_h$.

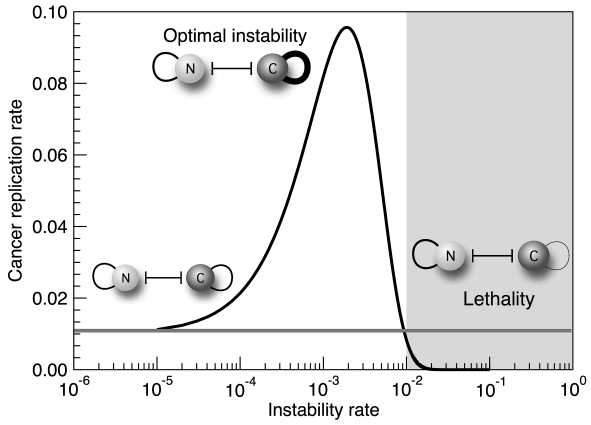

FIG. 1: Optimality and lethality in unstable cell populations. The vertical axis indicates the cancer replication rate against instability, as predicted from equation (5). The replication rate of normal cells is $r_0 = 0.01$ (in arbitrary units). The cancer population is assumed to be homogeneous. At low instability rates, competition between the two cell populations is symmetric and cancer coexists or slowly grows. The peak at the optimal rate μ_o is associated to the fastest potential growth of cancer. The grey area indicates the lethal phase, where excessive instability leads to a reduced proliferation of cancer cells, which are overcompeted by normal cells.

Considering Eq. (5) and the constant population constraint, it is possible to reduce the system of Eqs. (1)-(2) into a single equation describing the dynamics of the system in terms of the genetic instability μ. Thus, the cancer cell population is now captured by a logistic-like nonlinear equation:

$$\frac{dC}{dt} = r_n(\Gamma(\mu) - 1)C(1-C) \qquad (6)$$

Two fixed points are present: the zero-population one $C^* = 0$ and the maximum population state, here $C^* = 1$. It is easy to see that the first is stable if $\Gamma(\mu) < 1$ and unstable otherwise. By properly defining the function $\Gamma(\mu)$ we might be able to define the conditions under which genetic instability allows cancer growth to occur and overcome the host tissue. The critical mutation rate separating the two scenarios is sharp and defines a phase transition.

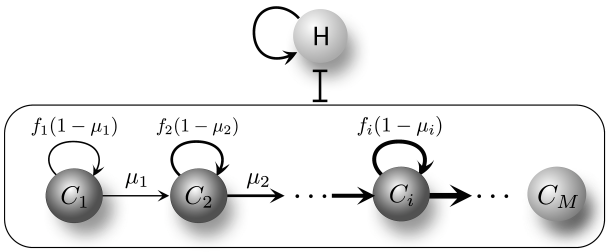

FIG. 2: Linear model of competition between normal cells (H) and a heterogeneous population of cancer cells, indicated as $C_1, C_2, ..., C_i$ which replicate with increasing rates f_i and mutate also at faster rates μ_i, as highlighted by the increasingly thick arrows. The effective replication rate of a given C_k compartment is $f_k(1-\mu_k)$.

The presence of a phase transition in this toy mean field model involving competition between two homogeneous populations offers an interesting prediction: further increases of instability can force cancer cells to enter the lethal phase. However, understanding how such shifts can occur requires a better understanding of the ways cancer cell populations evolve. Cancer cell populations are highly heterogeneous [44,45] and that means that we need to depart from the previous model approach.

III. LINEAR MODEL OF UNSTABLE CANCER

In an early paper [46] a discrete, sequential model of unstable cancer was introduced. The model considered a population of cancer cells having different levels of instability and competing among them and with the normal tissue (figure 2). This led to a description of M levels of instability describing an heterogeneous cancer cells population, which was governed by the following set of M differential equations:

$$\frac{dC_i}{dt} = f_{i-1}\mu_{i-1}C_{i-1} + f_i(1-\mu_i)C_i - C_i\Phi(H, \mathbf{C}), \quad (7)$$

where $i = 1, 3, ..., M$, $\mathbf{C} = (C_1, ..., C_M)$ and we consider the terms $\mu_0 = \mu_M = 0$ so that they properly define the first and last of the equations in (7). In the set (7), H indicates the host (healthy) population, whose dynamics would be described by an additional equation $dH/dt = f_H(H, C)$ which takes the general form

$$\frac{dH}{dt} = G(H) - H\Phi(H, \mathbf{C}) \qquad (8)$$

Here $G(H)$ introduces the explicit form of growth characterizing the normal tissue. A constant population constraint (CPC) was also introduced, namely a total constant population size $H + \sum_i C_i = 1$. This leads to an

explicit form of the competition ϕ function, namely

$$\Phi(H, \mathbf{C}) = G(H) + \sum_{k=1}^{M} f_k C_k \tag{9}$$

which is nothing but the average replication rate.

A numerical analysis of this system was performed for some parameter values, showing that the population dynamics of the cancer population spread over mutation space as a wave until a stable distribution (showing a single peak) around high instability levels was observed. However, no systematic analysis was performed in order to characterize potential phases and their implications. In particular, it was not studied the behavior exhibited by the heterogeneous population close to the optimal/lethal thresholds. Moreover, the linear model above is an oversimplification and a better description is needed in order to make reliable predictions.

IV. INTEGRAL EQUATION EXPANSION

The linear instability model reveals an important dynamical feature of unstable dynamics: a propagating front is formed and moves through instability space. Fronts (and their propagation dynamics) are a well known characteristic of many relevant biological processes [41,44,45] and can be analyzed in a systematic way through well known methods. Our first step here will be to convert the discrete model presented above into a more general, analytically tractable integral equation form. Such model will allow us exploring the phase space of our system and to make some analytic estimates of propagation speed.

An integral equation model can be derived starting from the previous linear model. Let us first notice that the equations (7) for C_i can be re-written as

$$\frac{dC_i}{dt} = \sum_{1}^{M} f_j C_j w_{ji} - C_i \Phi(H, \mathbf{C}). \tag{10}$$

This is done by introducing the following notation:

$$w_{ji} = \delta_{j,i-1}\mu_j + (1-\mu_j)\delta_{ij}, \tag{11}$$

and, as explained in the previous section, we consider the condition $\mu_0 = \mu_M = 0$ to properly describe the evolution of C_0 and C_M. An integral equation can be now constructed, using the continuous variable $C_i(t) = \Delta\mu \cdot c(\mu, t)$. Moreover, we need to generalize the functional connection between different instability levels, which was assumed to be a simple function in (7) but could adopt different forms. A general integral equation can be constructed, namely:

$$c(\mu, t+T) = c(\mu, t) + T \int_{-\mu}^{0} f(\mu+\Delta_\mu) c(\mu+\Delta_\mu, t) \omega(\Delta_\mu) d\Delta_\mu - c(\mu, t) T \phi(H, \mathbf{c}), \tag{12}$$

where we have used a continuous dispersal kernel $\omega(\Delta_\mu)$ [16,41,47] which provides the probability density that cancer cells in $c(\mu - |\Delta_\mu|, t)$ produce offspring, after a given time T, within the μ-coordinate i.e. further cells within the $c(\mu, t+T)$. Moreover, in Eq. (12) we have changed the notation of the average fitness from $\Phi(H, \mathbf{C})$ [as it appears in Eqs. (7) and (8)] in order to remark that we now use a continuous description for cancer cells. While in the linear model [Eqs. (7) and (8)] the average fitness depends on H and $\mathbf{C}$, in our integral model [Eq. (12)] the average fitness must depend on both H and the continuous distribution of cancer cells at time t (that we have writen as $\mathbf{c}$ to explicitly indicate its correspondence to $\mathbf{C}$ in the linear model).

Following analogous steps to those for cancer cells, we can also develop the differential Eq. (8) for healthy cells so that we obtain an explicit expression for the population H at time $(t+T)$. This yields:

$$H(t+T) = H(t) + T[G(H) - H\phi(H, \mathbf{c})] \tag{13}$$

The constant population requirement (defined above as $C + N = 1$ for the mean field model) can be expressed here as

$$H(t) + \int_0^M c(\mu, t) d\mu = 1 \tag{14}$$

$$H(t+T) + \int_0^M c(\mu, t+T) d\mu = 1 \tag{15}$$

and we assume that M is large enough so that we can ensure that $c(M, t) = 0$.

In this paper we will use this integral equation approach to describe our cancer quasispecies model. This model allows us to properly study the way the instability wave can (or cannot) propagate and some other phenomena including the catastrophic collapse of the cancer

population once the unstable wave crosses some given thresholds.

Using the previous condition and definitions, it is possible to develop our model equation. Let us indicate as $\phi = \phi(H, \mathbf{c})$, $f_H = G(H) - H\phi$ [which, considering Eq. (13), can be understood as the change in H cells per unit time], and compute the total cancer cells population as:

$$\Lambda(t) = \int_0^M c(\mu, t) d\mu. \tag{16}$$

Note that $\Lambda(t)$ strictly depends on (M, t), but the dependence on M has been omited because (as mentioned above) we consider M is high enough to satisfy the condition $c(M, t) = 0$. Thus, it is possible to see that our system is described by the following mathematical expressions:

$$T f_H + H + \Lambda(t) + T \int_0^M \int_{-\mu}^0 c(\mu + \Delta_\mu, t) f(\mu + \Delta_\mu) \omega(\Delta_\mu) d\Delta_\mu d\mu - T\phi\Lambda(t) = 1 \tag{17}$$

$$\Rightarrow 1 + TH\phi + T\phi\Lambda(t) = TG(H) + H + \Lambda(t) + \int_0^M T \int_{-\mu}^0 c(\mu + \Delta_\mu, t) f(\mu + \Delta_\mu) \omega(\Delta_\mu) d\Delta_\mu d\mu, \tag{18}$$

From the above equation (17) it is easy to derive the following expression for the average fitness of the population (that includes normal tissue and tumor cells):

$$\phi(H, \mathbf{c}) = G(H) + \int_0^M \int_{-\mu}^0 c(\mu + \Delta_\mu, t) f(\mu + \Delta_\mu) \omega(\Delta_\mu) d\Delta_\mu d\mu. \tag{19}$$

It is worth to note that the integro-difference equation (12) permits to analyze several dynamical properties of the system which cannot be attained by means of the previous linear model (10). In the linear model, the offspring of tumor cells in a given stage i may grow either in the same stage i or in the subsequent $i + 1$. A desirable feature of the continuous description from (12) is that the dispersal kernel can easily model different forms of instability-driven spread in the genetic landscape. In the following section, we analyze a simple case in which migration probability decays exponentially with the jumping distance Δ_μ. The linear model can also be recovered from Eq. (12) by introducing a dispersal kernel that restricts mutations to discrete points in the μ-space. In order to derive some analytical solutions of the system, such simplified dispersal kernels will be shown to be specially useful.

V. WAVE FRONTS IN INSTABILITY SPACE

In this section, we present several scenarios in which a tumor can either collapse or succeed over a healthy tissue. According to the integral model [Eqs. (12) and (19)], tumor evolution is mainly governed by competition. As explained above, this competition involves not only the fight between cancer cells and healthy cells, but also the struggle within cancer cell clones.

In the previous section we have presented a model that is mainly based on two dynamical features of tumors: replication (introduced by the growth function $f(\mu)$) and mutation (given by the dispersal kernel $\omega(\Delta_\mu)$). Concerning the replication process, below we consider some specific growth functions involving a constant reproduction rate for healthy cells, so that $G(H) = r_n H$. For tumor cells, the growth function depends on instability as $f(\mu) = r_n (1 + \alpha\mu) exp(-\mu/\mu_c)$. This was derived in [23] from the probabilistic condition defined by equation (5). The rate α introduces a selective advantage for cancer cells over healthy cells. The constant μ_c refers to a characteristic instability rate.

In order to model the mutant trend of cancer cells, let us consider the following continuous function for the dispersal kernel:

$$\omega(\Delta_\mu) = \frac{1}{\mu_{disp}} \exp\left(\frac{-|\Delta_\mu|}{\mu_{disp}}\right). \tag{20}$$

According to Eq. (20), a parent cell generates offspring at similar instability domains (i.e. situated at $\Delta_\mu \to 0$) with higher probability than new cells presenting much higher instability (i.e., living at $\Delta_\mu >> 0$). The parameter μ_{disp} represents a characteristic (within generation) instability increment. Since we have

$$\int_{-\infty}^0 \omega(\Delta_\mu) d\Delta_\mu = 1$$

the dispersal kernel distributes the cells of the new generation in the instability space, but it does not modify

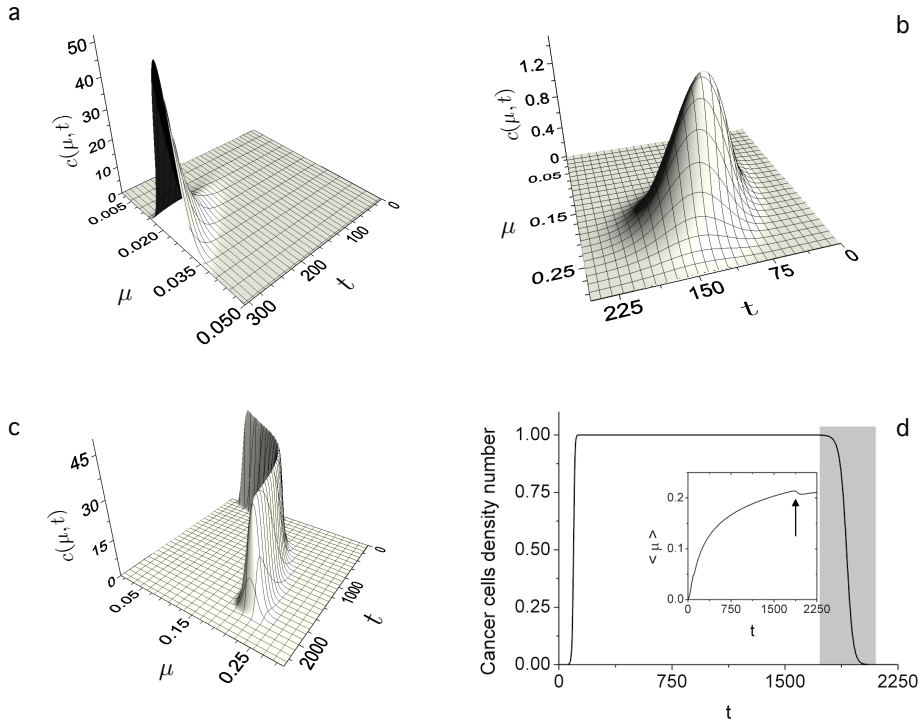

FIG. 3: The three major dynamical patterns of dynamical behaviour displayed by our mathematical model. Here the population density for different instability levels is plotted against instability and time. In (a), unstable tumours expand, evolving towards a stable, high instability rate. Time evolution for $r = 0.25, \alpha = 20$, $\mu_c = 0.08$ and $\mu_{disp} = 3 \cdot 10^{-4}$. Each time step is equivalent to a generation of cells. Cancer cells diffuse through the instability space as a wave. At early stages ($t < 200$), the fraction of cancer cells in the system is low. However, when cancer cells reach high enough instability (slightly above $\mu = 0.015$ in this example), a rapid increase in cancer population density is produced. (b) Tumor fails to get established. The following parameter values have been used: $r = 0.25$, $\alpha = 50$, $\mu_c = 0.08$ and $\mu_{disp} = 10^{-2}$. (c) Population collapse. Here expansion is followed by collapse after a long transient, as shown in (d). Here we have used $r = 0.25$, $\alpha = 50$, $\mu_c = 0.08$ and $\mu_{disp} = 1 \cdot 10^{-3}$.

the total number of cancer cells in the system.

A. Tumor wins phase

Figure 3a shows the evolution of a population of cancer cells which initially composes the 0.001% of the cells in the system. Cancer cells at $t = 0$ have been equally distributed within a range of low instability (namely, $\mu \in (0, 2 \cdot 10^{-4}]$). We observe an early stage ($t \in [0, 150]$) in which tumor cells remain at low values of the population density $c(\mu, t)$. Within this initial period, cancer cells do not overcome healthy cells because their selective advantage is not significant (i.e., $f(\mu) \simeq G(H)$ because $\mu \simeq 0$).

The dispersal kernel $\omega(\Delta_\mu)$ pushes forward the tumor population towards higher instability domains. In other words, at each time step a fraction of the cancer cells offspring becomes sensibly more unstable than their parent cells. A rapid increase in cancer cells population density is observed about $t = 200$ generations. The rapid growth affects cells whose genetic instability is above a certain threshold (see the region above $\mu = 1.5 \cdot 10^{-2}$). This indicates that such degree of instability provides for significant selective advantage over other cells in the system. During the fast growth phase, the population not only attains a large fraction of the total population, but it also continues migrating (see the left to right dispersion of the population wave). At the end of the time series in Fig. 3a, the concentration of cancer cells in the system is about 50% (we consider this condition is enough to cause the death of the host). This is an example of the dynamics at the cancer expansion phase.

B. Tumor failure phase

It seems reasonable to think that increasing the characteristic migration distance μ_{disp} should accelerate tumor proliferation, because cancer cells will reach optimal instability domains faster. However, increasing μ_{disp} does not necessarily lead to the tumor-win phase. It can actually jeopardize cancer propagation even when an already established population is formed. If a tumor cell produces

highly mutant descendants (i.e., new cells accumulating many new mutations) with high probability, it follows that the probability of generating descendants without additional mutations cannot be very large.

Figure 3b depicts an example of the tumor-failure phase. In this case the selective advantage presents a higher value (namely, $\alpha = 50$) than that for the tumor in the previous scenario. Here we observe a tumor population wave diffusing in the instability space, always coexisting with normal cells (the total number of cancer cells $\Lambda(t)$ do not exceed the 12% at any generation). Despite the relatively high selective advantage α, the high value of μ_{disp} prevents the tumor population to remain at the optimal instability domain, and hence cancer cells cannot grow fast. The tumor moves towards excessive instability, and cancer replication becomes smaller than that of the host tissue. These conditions define the tumor extinction phase.

C. Catastrophic tumor decay

A qualitatively different and somewhat unexpected outcome is displayed in Fig. 3c, where we have set a lower value of μ_{disp}. As a result, a fast extinction of healthy cells occurs and cancer cells invade all the available space before $t = 200$. Here we let the system evolve beyond the absence of healthy cells. Even if this situation typically involves the elimination of host cells, it could be observed in cell culture conditions. Moreover, we need to consider a potentially relevant situation, namely when a given tumor has expanded within large parts of the organ, as it occurs with many malignant cancers. After the rapid increase in cancer cells population density ($t \simeq 200$), the tumor continues its migration towards higher instability.

Since the value of μ_{disp} is relatively high, the tumor population is unable to stay within the optimal region. At every new generation, a large fraction of the progeny accumulates new mutations. The final outcome is very interesting: a collapse finally occurs. This is illustrated in figure 3d, where we plot the total cancer population and the average instability (inset) for the example of figure 3c. Around 1700 generations, cancer cells have accumulated so many mutations that they are almost unable to produce viable descendants. After $t = 2000$ there is no significant cancer cells population.

Despite the slow growth of $\langle\mu\rangle$, a catastrophic shift occurs, with a rapid decay of the tumor. Catastrophic shifts have been previously described within ecological and social systems [48] and are characterized by sudden system responses triggered by slow, continuous changes of given external control parameters. The novelty of our observation is that the changing parameter is affected by (and affects) population dynamics and thus is not externally tuned but internally increased.

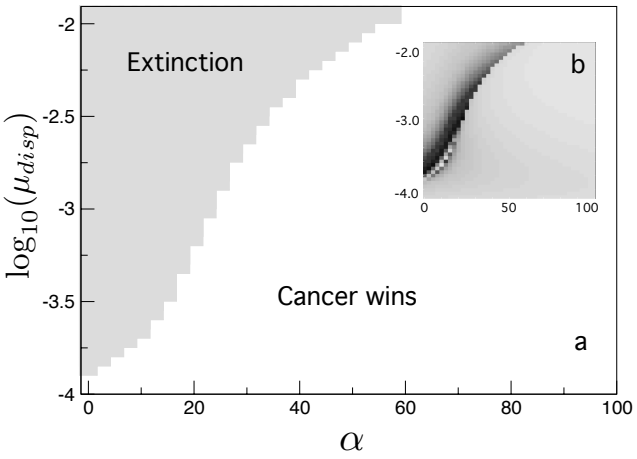

FIG. 4: Phases in the tumor growth model. The main plot (a) shows the two phases associated to the propagation (white) or extinction (gray) of the cancer cell population. The transition separating the two phases can be characterized by the transient dynamics exhibited by the model. The inset (b) displays the number of time steps (or cancer cells generations) to reach the corresponding final state represented in **a)**. Darker (lighter) zones are associated to longer (shorter) transients. As expected from a phase transition phenomenon, long transients are observed close to the boundary between both phases.

D. Phase space

A systematic exploration of the parameter space provides a picture of the two main phases, as shown in Fig. 4. The two axes involve a wide range of values for both α and μ_{disp}. In the first phase (gray squares), the tumor is driven to extinction. Extinction arises as a combination of two components: *i)* an insufficient fitness advantage of the early cancer cells (the cancer population progressively decays without reaching enough instability to develop), or *ii)* the tumor inability to keep the optimal instability (when this happens, a moderate population growth precedes the tumor failure). The second region (white area) stands for tumors that grow enough to overcome the healthy tissue.

The transition between the two regions is also marked by a rapid increase in the transient time. In Fig. 4b we have depicted the transient time steps (i.e., generations of cancer cells) to reach either the tumor extinction or its stable expansion to equilibrium values. As expected, longer times are needed near the phase transition.

VI. TUMOR FRONT SPEED

In the previous section, we have seen how some tumor population waves diffuse in the instability space. A relevant feature of propagating fronts, with direct importance for tumor growth, is the propagation speed of

the front. Such speed has been actually calculated for spatially growing tumors [17,49,50] and the front is thus a spatially defined one. Although we are here considering front propagation through instability space, the same reasoning applies. Here we derive an analytical, approximate solution for the front speed of the tumor. This will provide a quantitative measure of how fast cancer instability propagates. Since deriving an exact analytical expression for the front speed can be extremely cumbersome, some approximations are required.

First, let us consider early stages in tumor development (such as the first 150 in Fig. 3). Here the system is mostly composed of healthy cells, and few of cancer cells. This permits to approximate the complex expression for the average fitness [see Eq. (19)] as the reproduction rate of healthy cells, i.e.,

$$\phi(H, \mathbf{c}) \simeq G(H) \simeq r_n. \tag{21}$$

The second approximation we will consider refers to the dispersal kernel. According to Eq. (20) in the previous section, the dispersal kernel is a continuous function defined in the interval $[-\infty, 0]$. In this section we will consider the following simpler, discrete dispersal kernel:

$$\omega(\Delta_\mu) = 2p_e\delta(\Delta_\mu) + (1-p_e)\delta(\Delta_\mu + \mu_{disp})\gamma(\mu_{disp}), \tag{22}$$

where $\delta(\Delta_\mu)$ corresponds to the Dirac delta function operating on the variable Δ_μ, and $\gamma(\mu_{disp}) = 1$ if $\mu_{disp} \neq \mu$ and 2 otherwise [51].

The above discrete kernel (22) considers that every new cell can either stay at the same instability μ of the parent cell (with probability p_e, which is called persistence) or jump into a higher instability $\mu + \mu_{disp}$ [with probability $(1 - p_e)$]. Although the discrete kernel (22) is much simpler than the continuous kernel (20), it also models a major feature in cancer cells replication (see the previous section), that is: the stronger the mutant trend of cancer cells, the weaker the ability of the population to keep an optimal instability.

Thus, according to Eqs. (21) and (22) above, our approximation to Eq. (12) reads:

$$c(\mu, t+1) = c(\mu, t) + \int_{-\mu}^{0} f(\mu + \Delta_\mu)c(\mu + \Delta_\mu, t)(2p_e\delta(\Delta_\mu) + (1 - p_e)\delta(\Delta_\mu + \mu_{disp})\gamma(\mu_{disp}))d\Delta_\mu - c(\mu, t)r_n. \tag{23}$$

Taking into account the integrative properties of the Dirac delta function $\delta(\Delta_\mu)$, the above equation 23 can be rewritten in terms of a much simpler functional form:

$$c(\mu, t+1) = c(\mu, t) + p_e c(\mu, t)f(\mu) + (1 - p_e)c(\mu - \mu_{disp}, t)f(\mu - \mu_{disp}) - c(\mu, t)r_n, \tag{24}$$

where we have assumed that the condition $\mu \geq \mu_{disp}$ holds, since we are interested in the propagation of the tumor front. Indeed, for $\mu < \mu_{disp}$ cancer cells evolve as in Eq. (24) but neglecting the third term on the RHS. The front speed from reaction-dispersal integro-difference equations such as (12) can be obtained under some general assumptions [16,17] associated with the shape to be expected for the propagating front.

Here we are interested in the simplified version (24) of the model. Thus we only need to assume that there exist constant shape solutions of the form

$$c(\mu, t) = c_0 \exp\left[-\lambda z\right]$$

for large values of the coordinate $z \equiv (\mu - vt)$.

This yields the following approximate, analytic relation between the tumor front speed and the wave front shape parameter λ:

$$v(\lambda) = \frac{1}{\lambda} \ln\left[p_e f(\mu) + (1 - p_e)f(\mu - \mu_{disp})e^{\lambda\mu_{disp}} - r_n + 1\right]. \tag{25}$$

Finally, by means of the standard, marginal stability condition [16] the minimal speed $v_* = \min_{\lambda>0} v(\lambda)$ is the one

selected by the front. In the analysis below, the following method has been used to find the value of the approximate speed v_*. First, we plotted the numerical solution to Eq. (25) on the $\lambda > 0$ axis. As usual, we obtain a function $v(\lambda)$ that is convex from below [16]. Thus, we look for the minimum value of this function, which reveals the approximate value for the front speed of the tumor as it propagates through instability space (i.e., v_*).

The approximate front speed v_* should not be taken as a general trend in tumor evolution, since it is subject to the approximations explained above. Indeed, for cases in which healthy cells overcome the tumor it eventually predicts negative values of the front speed. However, predicting a negative front speed can also be seen as the retreat (i.e., the death) of the cancer population (which at early times is only composed by a few cancer cells with $\mu \to 0$). Nevertheless, the approximate speed v_* provides remarkably good results for the front speeds of lethal tumors (i.e., for tumors within the parameter region in which the tumor succeeds), as we show in Fig. 5.

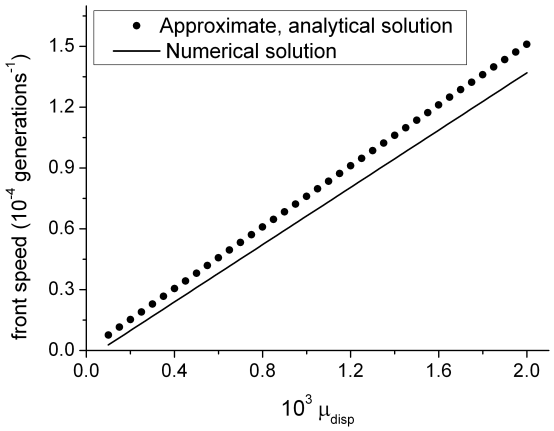

FIG. 5: Front speed of the cancer population travelling on the instability space, as a function of the characteristic dispersal distance μ_{disp}. The line and the circles stand for the numerical results and the approximate analytical speed v_*, respectively. The rest of the parameters used to compute the front speed are: $r_n = 0.25$, $\alpha = 20$, $p_e = 0.85$ and $\mu_c = 0.08$.

Fig. 5 shows a comparison between the numerical and the approximate analytical speed v_* for the tumor front speed as a function of the characteristic dispersal distance μ_{disp}. Numerical solutions for the front speed have been computed by numerically solving [52] the model Eqs. (12) and (19) using the discrete version of the dispersal kernel (22). For both the numerical and the approximate analytical solutions, the front speed monotonically increases with the characteristic distance μ_{disp}. As far as the order of magnitude is concerned, the approximate analytical speed v_* is able to predict the more exact numerical results for the tumor front speed. Furthermore, relative differences (which are typically above 15%) between the analytical results and the numerical solutions are approximately independent of μ_{disp}.

The solutions for the front speed on the instability space in Fig. 5 exhibit an approximately linear dependence on the characteristic dispersal distance μ_{disp}. Since the instability μ of tumor cells is directly related with the selection of cells during tumor evolution, μ_{disp} can also be interpreted as a parameter that determines the selective intensity on cancer cells. Previous models on adaptive front waves have also yielded adaptation speeds that depend on selective intensity parameters. In this context, in [14] the speed of adaptation for asexual clones that compete for space scales as $\mu^{1/2}$ in one-dimensional habitats and $\mu^{1/3}$ in two-dimensional ones (in their model, μ stands for the rate at which new mutations appear at each lattice site). Also, in Ref. [53] the authors found that, when a continuous two-dimensional space is considered, genetic wave speeds are proportional to $s^{1/2}$, where s represents the small fitness effects s of beneficial mutations. In our model we have studied the front speed of the tumor on the instability space, without taking into account neither spatial structure nor the physical environment. However, both μ and μ_{disp} have similar interpretations to the selective parameters in Refs. [14,53]. Future work could be directed to introduce spatial effects into our model, and it would be interesting to explore if similar scaling exponents arise in the dependence of the tumor invasion speed and genetic instability rates.

VII. DISCUSSION

In this paper we have presented an integral model for the evolution of unstable tumors. Our model improves a previous compartment description of the cancer cells population, because we consider the genetic instability as a continuous variable that characterizes the state of the cell. The model considers a population of tumor cells that replicate and migrate (mutate) in the instability space, while competing for available resources (a limited population constraint has been applied). This model is based on several simplifying assumptions, from the linear nature of interactions between instability levels to the dispersal kernels used.

We have presented an extended analysis of unstable cancer evolution over the two most relevant parameters of the model: the selective advantage of cancer cells over the healthy cells population, and the characteristic migration distance within instability space (which determines the mutant tendency of cancer cells). Several outcomes of the process have been found. Two of them are expected: either the growth or the failure of cancer to succeed are predicted by the simplest mean field model that can be defined, as discussed in section II. The integral equation approach confirms such prediction, although it allows to substantiate it in more accurate ways, providing a formal framework to calculate useful quantities, particularly the front speed of our population through the μ-space.

Moreover, this formal approach provides a natural way to properly introduce population heterogeneity.

An additional scenario has also been found, namely the catastrophic shift phase, where the tumor grows, eventually expanding over a significant part of the total available space, with a steady growth of instability. However, at some point the excessive instability level leads to a population collapse, with no cancer cells in the end. Our model does not consider immune components or other biologically relevant factors [54]. Instead, the key factor responsible for the tumor collapse is high genetic instability. This result provides further support to the original proposal that lethal thresholds of instability exist in cancer [23,24] which could be exploited for therapeutic purposes, even when major success of the cancer population is observable. Future work should further explore this observation, adding also other known threats to cancer progression, such as starvation or hypoxia, which could further enhance the frequency and sharpness of these thresholds.

Acknowledgments

We thank the members of the CSL for useful discussions. This work was supported by grants from the Fundacion Botin, a MINECO grant and the Santa Fe Institute.

VIII. REFERENCES

1. M. Greaves and C. C. Maley, Nature **481**, 306 (2012).
2. L. M. F. Merlo, J. W. Pepper, B. J. Reid and C. C. Maley, Nature Rev Cancer **6**, 924 (2006).
3. B. Vogelstein and K. W. Kinzler, Nature Medicine **10**, 789 (2004).
4. D. P. Cahill, K. W. Kinzler, B. Vogelstein and C. Lengauer, Trends Genet. **15**, M57 (1999).
5. M. Chow and H. Rubin, Cancer Res. **60**, 6510 (2000).
6. J. Jackson L. A. Loeb Genetics **148**, 1483 (1998).
7. C. Lengauer, K. W. Kinzler and B. Vogelstei, Nature **396**, 643 (1998).
8. L. A. Loeb, Cancer Res. **51**, 3075 (1991).
9. L. A. Loeb, Cancer Res. **54**, 5059 (1994).
10. B. Vogelstein, N. Papadopoulos, V. E. Velculescu, S. Zhou, L. A. Diaz Jr. and K. W. Kinzler, Science **339**, 1546 (2013).
11. F. Michor, Y. Iwasa and M. A. Nowak, Nat. Rev. Cancer **4**, 197 (2004).
12. N. Beerenwinkel, T. Antal, D. Dingli, A. Traulsen, K. Kinzler, V. E. Velvulescu, B. Vogelstein and M. A. Nowak, PLOS Comp. Biol. **3**, e225 (2007).
13. R. V. Solé and J. Bascompte, *Self-Organization in Complex Ecosystems* (Princeton U. Press, Princeton, New Jersey, 2007).
14. E.A. Martens and O. Hallatschek, Genetics **189**, 1045 (2011).
15. E.A. Martens, R. Kostadinov, C. C. Maley and O. Hallatschek, New J. Phys. **13**, 115014 (2011).
16. J. Fort and T. Pujol, Rep. Prog. Phys. **71**, 086001 (2008).
17. J. Fort and R. V. Solé, New J. Phys. **15**, 055001 (2013).
18. E. Khain, L. M. Sander, and A. M. Stein, Complexity **11**, 53 (2005).
19. R. A. Gatenby and E. T. Gawlinski, Cancer Res. **56**, 5745 (1996).
20. S. Negrini, V. G. Gorgoulis and T. D. Halazonetis, Nat. Rev. Mol. Cell Biol. **11**, 220 (2010).
21. R. A. Gatenby and B. R. Frieden, Cancer Res. **62**, 3675 (2002).
22. R. A. Gatenby and B. R. Frieden, Mutat. Res. **568,** 259 (2004).
23. R. V. Solé, Europ. J. Phys. B **35**, 117 (2003).
24. R. V. Solé and T. Deisboeck, J. Theor. Biol. **178**, 47 (2004).
25. J. M. Coffin, Science **267**, 483 (1995).
26. E. Domingo, J. J. Holland, C. Biebricher and M. Eigen, in: *Molecular Evolution of the Viruses*, edited by A. Gibbs, C. Calisher and F. Garcia-Arenal (Cambridge U. Press, Cambridge, 1995).
27. Domingo, E. and Holland, J. J. in: *The evolutionary biology of RNA viruses*, pp. 161-183, edited by S. Morse (Raven Press, New York, 1994).
28. M. Eigen, Naturwiss. **58**, 465 (1971).
29. M. Eigen, J. McCaskill and P. Schuster, Adv. Chem. Phys. **75**, 149 (1987).
30. P. Schuster, in: *Complexity: metaphors, models and reality*, pp. 383-418, edited by G. A. Cowan, D. Pines and D. Meltzer (Addison-Wesley, Reading, MA 1994).

31. S. Cottry, C. E. Cameron, and R. Andino, Proc. Natl. Acad. Sci. USA **98**, 6895 (2001).

32. L. A. Loeb, J. M. Essigmann, F. Kazazi, J. Zhang, K. D. Rose and J. I. Mullins, Proc. Natl. Acad. Sci. USA **96**, 1492 (1999).

33. J. J. Holland, E. Domingo, J. C. de la Torre and D. A. Steinhauer, J. Virol. **64**, 3960 (1999).

34. P. R. A. Campos and J. F. Fontanari, PRE **58**, 2664 (1998).

35. P. Tarazona, Phys. Rev. A **45**, 6038 (1992).

36. P. J. Gerrish, A. Colato, A. S. Perelson , and P. D. Sniegowski, PNAS **104**, 6266 (2007).

37. L. A. Loeb, Nat. Rev. Cancer **11**, 450 (2009).

38. Q. Zhang and R. H. Austin, Annu. Rev. Cond. Mat. Phys **3**, 363 (2012).

39. R. Pastor-Satorras and R. V. Solé, Phys. Rev. E **64**, 051909 (2001).

40. D. B. Saakian, E. Munoz, C. K. Hu, and M. W. Deem. Phys. Rev. E **73**, 041913 (2006).

41. V. Ortega-Cejas, J. Fort and V. Mendez, Ecology **85**, 258 (2004).

42. E. Eisenberg and E. Y. Levanon, Trends Genet. **19**, 362 (2003).

43. P. A. Futreal, L. Coin, M. Marshall, T. Down, T. Hubbard, Richard Wooster, N. Rahman and M. R. Stratton, Nature Rev. Cancer **4**, 177 (2004).

44. I. Gonzalez-Garcia, R. V. Solé and J. Costa, Proc. Natl. Acad. Sci. USA **99**, 13085 (2001).

45. A. Marusyk, V. Almendro, K. Polyak, Nat. Rev. Cancer **12**, 323 (2012).

46. R. V. Solé, C. Rodriguez-Caso, T. Deisboeck, and J. Saldanya, J. Theor. Biol. **253**, 629 (2008).

47. N. Isern, J. Fort and J. Pérez-Losada, J. Stat Mech: Theor Exp **10**, P10012 (2008).

48. M. Scheffer, *Critical transitions in Nature and Society* (Princeton U Press, New York 2009); R. Solé, *Phase Transitions* (Princeton U Press, New York, 2011).

49. K. R. Swanson, C. Bridge, J. D. Murray, and J. E. C. Alvord, J. Neurol. Sci. **216**, 1 (2003).

50. K. R. Swanson, J. E. C. Alvord, and J. D. Murray, Math. Comp. Modell. **37**, 1177 (2003).

51. Note that the 2 factors in Eq. (22) provide the necessary corrections in case the arguments of the Dirac delta functions in Eq. (22) coincide with the integration limits in Eqs. (12) or (24). On the one hand, the factor 2 appearing explicitly in Eq. (22) is necessary for the dispersal kernel to satisfy the condition $\int_{-\infty}^{0} \omega(\Delta_\mu) d\Delta_\mu = 1$ (see Section V). For an analogous reason we consider the factor 2 in $\gamma(\mu_{disp})$, so that cells at $c(\mu_{disp}, t+1)$ receive the proper fraction [i.e., $(1-p_e)$ instead of $(1-p_e)/2$] from the parent cells at $c(0,t)$.

52. When numerically solving the integral model, the position of the edge of the front can be obtained for each generation (time step). The numerical solutions for the front speed (Fig. 5) have been obtained by linear regression of the time-dependent position of the front. For proper comparison, all the analytical solutions and the numerical results in Fig. 5 have been computed at transient times such that the edge of the front is close to $\mu = 0.01$.

53. E. S. Claudino, M. L. Lyra and I. Gleria, Phys. Rev E **87**, 032711 (2013).

54. R. P. Garay and R. Lefever, J. Theor. Biol. **73**, 417 (1978).